# Formation of metastable $dt\mu$ molecules in $t\mu(2s)$-$D_2$ collisions

J. Wallenius and P. Froelich
*Department of Quantum Chemistry, Box 518, S-751 20 Uppsala, Sweden*
(Received 4 December 1995)

The formation process of metastable $dt\mu$ molecules in $D_2$-$T_2$ mixtures is investigated. The $dt\mu$ molecule exhibits a series of three-body resonances embedded in the $t\mu+d$ scattering continuum just below the $t\mu(2s)+d$ threshold. These states can be formed in collisions of *excited* $t\mu(2s)$ atoms with $D_2$ molecules, whereby the excess of binding energy is absorbed by the rovibrational degrees of freedom of $D_2$. We present a scattering-theoretic model for this process, and perform a numerical calculation of its cross section. The essential transition amplitudes are obtained from three-body wave functions for the $dt\mu$ subcluster, and adiabatic wave functions for the entire hybrid system in the final channel. It is found that the effective formation rate is limited by the Auger-transition rates of the molecular complex formed. The calculated cross sections exhibit broad ''peaks,'' with magnitudes large enough for the formation process to favorably compete with deexcitation of $t\mu(n=2)$ atoms via radiative and collisional processes. The formation of metastable $dt\mu$ can therefore be one of the fastest processes depleting the $n=2$ levels of the $t\mu$ atom in hydrogen mixtures, of importance for low-energy muon science, electroweak physics, and muon catalyzed fusion. [S1050-2947(96)03107-1]

PACS number(s): 36.10.−k, 03.80.+r, 33.15.−e

## I. INTRODUCTION

Muon catalyzed fusion ($\mu$CF) as we know it today is supposed to proceed mainly via the bound states of the $dt\mu$ molecule with angular momentum $J=0$ [1]. There are several reasons for this, notably (i) although the muons enter the $\mu$CF cycle in highly excited states of the muonic atoms $d\mu$ and $t\mu$ with main quantum number $n\simeq 11$ [2], within $t=10^{-11}$ s they will cascade down to the $t\mu(1s)$ ground state via various deexcitation and transfer processes. (ii) The so-called Vesman mechanism [3] facilitates a very effective formation of $dt\mu$ molecules in collisions of $t\mu(1s)$ with $D_2$ or $DT$ molecules. (iii) Even though the loosely bound state formed by Vesman's mechanism is of angular momentum $J=1$, subsequent Auger transitions prompts $dt\mu$ in fast fusing ($\lambda_f=1.2\times 10^{12}\ \mathrm{s}^{-1}$) bound states of angular momentum $J=0$.

However, recent investigations have demonstrated that the bound (or *de facto* semibound) spectral structure of $dt\mu$ is richer than expected. A series of metastable states below the $t\mu(2s)+d$ threshold that may be associated with the adiabatic $3\sigma$ potential has been discovered [4–7]. If these states, from now on labeled $dt\mu$*, are formed during the cascade of the $dt\mu$ cycle they will decay into highly energetic $d\mu(1s)$ or $t\mu(1s)$ atoms [8]. The decay into $d\mu(1s)$ is expected to increase the fraction $P_{1s}^{d\mu}$ of muons reaching the ground state of $d\mu$ atoms and holds the potential for removal of the persisting disagreements between the experiment and theory regarding the precise values of $P_{1s}^{d\mu}$ [9].

In order to be definite about the influence of the side path thus appearing in the muon catalyzed fusion cycle, it is necessary to evaluate excited-state scattering cross sections to a higher degree of precision. In what follows we will present a detailed scattering-theoretic model for the process of formation of metastable muonic molecules in collisions between excited muonic atoms and hydrogen molecules.

In Sec. II the theoretical framework is given, leading to a Breit-Wigner cross section featuring two essential components, the entrance width and the reactive width. In Sec. III relevant energy levels and wave functions of $dt\mu$* are calculated, while Sec. IV is concerned with the evaluation of the reactive width. In Sec. V effective formation cross sections are calculated, leading to estimations of $\lambda_{dt\mu*}^{\mathrm{eff}}$. The credibility of our model is tested by evaluation of well-known entrance widths for the formation of *bound* states of $dd\mu$ and $dt\mu$.

## II. THE FORMATION PROCESS

The interesting feature of muonic molecule formation is that it may occur as a virtual (i.e., intermediate) process in the $t\mu(2s)$ collision, without participation of a third body. Indeed, the formation event may be related to the ''first step'' of the higher-order scattering process proceeding via intermediate molecular states, including resonances. The transition matrix element for $t\mu(2s)+d$ scattering is given, in the ''prior'' form, by

$$\begin{aligned} T_{fi}(E) &= \langle \psi_f^{(-)} | V_i | \phi_i \rangle \\ &= \left\langle \phi_f \middle| V_i + V_f \frac{1}{E-H+i\epsilon} V_i \middle| \phi_i \right\rangle \\ &= \langle \phi_f | V_i | \phi_i \rangle + \int \sum \frac{\langle \phi_f | V_f | \phi_r \rangle \langle \phi_r | V_i | \phi_i \rangle}{E-E_r+i\epsilon}, \end{aligned} \tag{1}$$

where $V_i, V_f$ specify the initial and final channel interactions, $\phi_i, \phi_f$ are the initial and final free waves describing the channel motion with relative collision energies $E_i$, $E_f$, respectively, and $\psi_f^{(-)}, \psi_i^{(+)}$ are the scattering solutions to the full Hamiltonian $H$. The summation is over the discrete

 

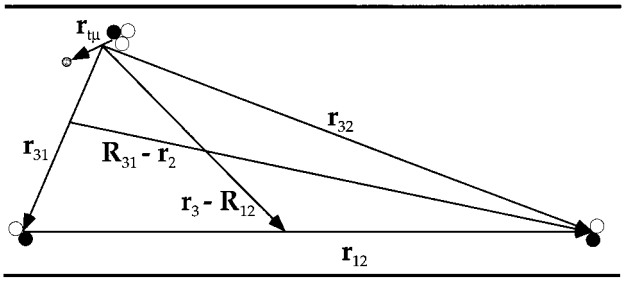


FIG. 1. Coordinates of the $\langle t\mu - D_2 \rangle$ system.

spectrum of $H$, which in our approach includes also the resonant states. The transition amplitude consists of a direct and a resonant term of which only the latter is relevant for the formation process considered here. The quantity $|\langle \phi_r | V_i | \phi_i \rangle|^2$ is called the partial width for *entering* the resonance from channel $i$, while $|\langle \phi_f | V_f | \phi_r \rangle|^2$ is the partial width for *leaving* the resonance and going to channel $f$ [10]. The first step of the nondirect scattering process dictates the size of the ''entrance width'' for the formation of the resonant state $\phi_r$.

We notice that the resonance formation may occur not only during the elastic scattering ($E_i = E_f, V_i = V_f$),

$$t\mu(2s) + d \rightarrow t\mu(2s) + d, \tag{2}$$

but also during the direct deexcitation process ($E_i \neq E_f, V_i = V_f$)

$$t\mu(2s) + d \rightarrow t\mu(1s) + d, \tag{3}$$

which may also occur with muon transfer ($E_i \neq E_f, V_i \neq V_f$)

$$t\mu(2s) + d \rightarrow d\mu(1s) + t. \tag{4}$$

This is because the resonances below the $t\mu(2s)$ threshold connect the entrance channel with two energetically open arrangement channels with lower thresholds, namely $t\mu(1s) + d$ and $d\mu(1s) + t$. Hence the formation can be viewed as the first step of the above-mentioned processes, with the entrance width in all cases given by

$$\Gamma = 2\pi |\langle \phi_r | V_i | \phi_i \rangle|^2. \tag{5}$$

The matrix element in Eq. (5) is ''off the energy shell'' in that it connects the initial state in the entrance channel $[t\mu(2s) + d]$ of the molecular continuum with the (under-threshold) metastable state with total energy $E_r \leq E$. Here we assume that, in analogy with the ground-state case, the formation is facilitated by a third body, which absorbs the excess of the binding energy. Since several of the resonances are located within the dissociation energy of $D_2$ ($\simeq 4.5$ eV) below the $t\mu(2s)$ threshold, we will consider the Vesman mechanism [3] as a third body interaction, whereby the excess of binding energy is transferred to the rovibrational degrees of freedom of the hybrid $[(dt\mu^*)dee]$ molecule in the process

$$t\mu(2s) + D_2 \rightarrow [(dt\mu^*)dee]_{\nu K} \tag{6}$$

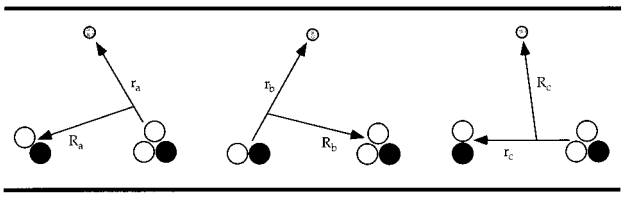


FIG. 2. The three rearrangement channels of the $dt\mu$ system and their Jacobian coordinates.

with $\nu$ being the vibrational and $K$ the rotational quantum number of the hybrid molecule. The cross section for the above reaction is given by the Breit-Wigner relation

$$\sigma(E_{\rm coll}) = \frac{\pi}{k^2} \frac{\Gamma_{\rm ent}\Gamma_r}{(E_{\rm coll} - E_{\rm res})^2 + \frac{1}{4}(\Gamma_{\rm ent} + \Gamma_r)^2} \tag{7}$$

with the Vesman resonant energy $E_{\rm res}$ satisfying the energy conservation condition

$$E_{\rm res} + E_b^{vJ} = \Delta E_{\rm rovib} + \Delta E_{\rm hf}, \tag{8}$$

where $E_b^{vJ}$ is the binding energy with respect to the $t\mu(2s)$ threshold of the metastable molecular state labeled by vibrational and rotational quantum numbers $v$ and $J$. $\Delta E_{\rm rovib}$ is the difference between the rovibrational levels of the hybrid molecule $[(dt\mu^*)dee]_{\nu K}$ and the $D_2$ molecule ground state, while $\Delta E_{\rm hf}$ is the difference in hyperfine splitting between $t\mu$ and $dt\mu$ levels.

$\Gamma_r$ is the reactive scattering width, given by

$$\Gamma_r = \Gamma_A + \Gamma_f + \Gamma_c + \Gamma_\gamma. \tag{9}$$

Here, $\Gamma_A$ is given by the rate of Auger deexcitations of the metastable molecule, $\Gamma_f$ is the fusion width, while $\Gamma_c$ and $\Gamma_\gamma$ are the widths for Coulombic and radiative decay into either $d\mu(1s) + t$ or $t\mu(1s) + d$.

The entrance width $\Gamma_{\rm ent}$ is discussed in Appendix A. There we derive the following formulas, equivalent to the ones obtained from $R$-matrix theory by Lane [11]:

$$\Gamma_{\rm ent} = \frac{4mk}{(4\pi)^2} \sum_M \int d\hat{k} |N(\boldsymbol{k})|^2 \tag{10}$$

$$N(\boldsymbol{k}) \equiv \langle \overline{\Psi}_{\nu K}(\boldsymbol{R}_{31} - \boldsymbol{r}_2) \Phi_{JM_J}(\boldsymbol{r}_{31}, \boldsymbol{r}_{t\mu}) \times |V_{31}| \Psi_{0K_i}(\boldsymbol{r}_{12}) \eta_{2s}(\boldsymbol{r}_{t\mu}) e^{i\boldsymbol{k}\cdot(\boldsymbol{r}_3 - \boldsymbol{R}_{12})} \rangle. \tag{11}$$

In the above expression, the final wave function of the entire system is written in a product approximation. In the initial channel ($\phi_i$), $\Psi_{0K_i}$ is a wave function describing the nuclear motion of $D_2$ in the electronic Born-Oppenheimer (BO) potential, $\eta_{2s}$ is the atomic wave function of $t\mu$, and the relative motion of $D_2$ with respect to $t\mu$ is described by a plane wave of momentum $k$. In the reaction channel ($\phi_r$), $\Psi_{\nu K}$ is a BO wave function describing the motion of $d$ with respect to $dt\mu$ treated as a point charge, and $\Phi_{JM_J}(\boldsymbol{r}_{31}, \boldsymbol{r}_{t\mu})$ is the complete three-body wave function of quasibound $dt\mu$ of angular momentum $J$. The sum over $M$ is to be taken over the magnetic quantum numbers $M_J$ and $M_K$. Coordinate la-

beling is explained in Fig. 1. $V_{31}$ is the three-body potential acting between the $t\mu$ atom and the target nucleus, while the interaction $V_{32}$ between the $t\mu$ atom and the spectator nucleus has been neglected.

Atomic units $m_e=\hbar=e=1$ are used throughout this paper if not otherwise explicitely stated. It is convenient to express the other coordinates in terms of $\boldsymbol{r}_{31}$ and $\boldsymbol{R}\equiv\boldsymbol{R}_{31}-\boldsymbol{r}_2$.

Defining the projection coefficients

$$f=\frac{m_1(m_1+m_2+m_3)}{(m_1+m_2)(m_1+m_3)},\quad g=\frac{m_2}{m_1+m_2},\quad h=\frac{m_3}{m_1+m_3} \tag{12}$$

we have

$$\Psi_{0K_i}(\boldsymbol{r}_{12})e^{i\boldsymbol{k}\cdot(\boldsymbol{r}_3-\boldsymbol{R}_{12})}\equiv\Psi_{0K_i}(\boldsymbol{R}-h\boldsymbol{r}_{31})e^{i\boldsymbol{k}\cdot(f\boldsymbol{r}_{31}+g\boldsymbol{R})}.$$

If one assumes that the range of $\boldsymbol{r}_{31}$ integration, determined by the factor $V_{31}\Phi_{JM_J}(\boldsymbol{r}_{31},\boldsymbol{r}_{t\mu})$, is much less than the range of $\boldsymbol{R}$, then an approximation for $\Psi_{0K_i}$ comes from the first terms of its Taylor expansion:

$$\Psi_{0K_i}(\boldsymbol{R}-h\boldsymbol{r}_{31})\simeq\Psi_{0K_i}(\boldsymbol{R})-h\boldsymbol{r}_{31}\cdot\nabla\Psi_{0K_i}(\boldsymbol{R}) \tag{13}$$

and $N(\boldsymbol{k})$ becomes

$$\begin{aligned}N(\boldsymbol{k})\simeq&\langle\Phi_{JM_J}(\boldsymbol{r}_{31},\boldsymbol{r}_{t\mu})|V_{31}|\,\eta_{2s}(\boldsymbol{r}_{t\mu})e^{if\boldsymbol{k}\cdot\boldsymbol{r}_{31}}\rangle\langle\overline{\Psi}_{\nu K}(\boldsymbol{R})|\Psi_{0K_i}(\boldsymbol{R})e^{ig\boldsymbol{k}\cdot\boldsymbol{R}}\rangle\\&-h\langle\Phi_{JM_J}(\boldsymbol{r}_{31},\boldsymbol{r}_{t\mu})|V_{31}|\boldsymbol{r}_{31}\eta_{2s}(\boldsymbol{r}_{t\mu})e^{if\boldsymbol{k}\cdot\boldsymbol{r}_{31}}\rangle\cdot\langle\overline{\Psi}_{\nu K}(\boldsymbol{R})|\nabla\Psi_{0K_i}(\boldsymbol{R})e^{ig\boldsymbol{k}\cdot\boldsymbol{R}}\rangle.\end{aligned} \tag{14}$$

In order to reduce the complexity of expression (14) we choose to investigate it for $K_i=0$. We then have

$$\begin{aligned}N(\boldsymbol{k})\simeq&\langle\Phi_{JM_J}(\boldsymbol{r}_{31},\boldsymbol{r}_{t\mu})|V_{31}|\,\eta_{2s}(\boldsymbol{r}_{t\mu})e^{if\boldsymbol{k}\cdot\boldsymbol{r}_{31}}\rangle\langle\overline{\psi_\nu}(R)Y_{KM_K}(\hat{\boldsymbol{R}})|\psi_0(R)Y_{00}(\hat{\boldsymbol{R}})e^{ig\boldsymbol{k}\cdot\boldsymbol{R}}\rangle\\&-h\langle\Phi_{JM_J}(\boldsymbol{r}_{31},\boldsymbol{r}_{t\mu})|V_{31}|\boldsymbol{r}_{31}\eta_{2s}(\boldsymbol{r}_{t\mu})e^{if\boldsymbol{k}\cdot\boldsymbol{r}_{31}}\rangle\cdot\left\langle\overline{\psi_\nu}(R)Y_{KM_K}(\hat{\boldsymbol{R}})\middle|\hat{R}\frac{\partial\psi_0}{\partial R}Y_{00}(\hat{\boldsymbol{R}})e^{ig\boldsymbol{k}\cdot\boldsymbol{R}}\right\rangle,\end{aligned} \tag{15}$$

where $\psi_\nu$ is the vibrational part of the (BO) $D_2$ wave functions

$$\Psi_{00}(\boldsymbol{R})=\psi_0(R)Y_{00}(\hat{\boldsymbol{R}}),\quad \overline{\Psi}_{\nu K}(\boldsymbol{R})=\overline{\psi_\nu}(R)Y_{KM_K}(\hat{\boldsymbol{R}}). \tag{16}$$

The muonic matrix elements (in the $\boldsymbol{r}_{31}$ space) are calculated using the property (see Appendix B)

$$\begin{aligned}&\langle\Phi_{JM_J}(\boldsymbol{r}_{31},\boldsymbol{r}_{t\mu})|V_{31}|\,\eta_{2s}(\boldsymbol{r}_{t\mu})e^{if\boldsymbol{k}\cdot\boldsymbol{r}_{31}}\rangle\\&\quad\simeq\beta\langle\chi_{\upsilon J}(r_{31})Y_{JM_J}(\hat{\boldsymbol{r}}_{31})|E_b^{\upsilon J}|e^{if\boldsymbol{k}\cdot\boldsymbol{r}_{31}}\rangle\end{aligned} \tag{17}$$

with

$$\beta=\langle\Phi_{JM_J}(\boldsymbol{r}_{31},\boldsymbol{r}_{t\mu})|\,\eta_{2s}(\boldsymbol{r}_{t\mu})\rangle_{\boldsymbol{r}_{t\mu}} \tag{18}$$

and $\chi_{\upsilon J}(\boldsymbol{r}_{31})$ is the pseudo wave function obtained by integrating $\Phi_{JM_J}$ over the muon coordinate.

Details of the integration over angles $\hat{\boldsymbol{r}}_{31}$ and $\hat{\boldsymbol{R}}$ in (15) are given Appendix C, resulting in formula (C6). Defining the radial matrix elements

$$\begin{aligned}&T_{\upsilon J}^{\mu L}\equiv\beta\langle\chi_{\upsilon J}(r_{31})|E_b^{\upsilon J}|r^L j_{|J-L|}(fkr_{31})\rangle,\\&T_{\nu K_\pm}^{eL}\equiv\left\langle\overline{\psi_\nu}(R)\middle|j_{|K\pm L|}(gkR)\left(\frac{d}{dR}\right)^L\psi_0(R)\right\rangle\end{aligned} \tag{19}$$

$\Gamma_{\rm ent}^{JK}(k)$ is evaluated by squaring expression (C6), integrating over angles $\hat{\boldsymbol{k}}$ and taking the sum over $M_J$ and $M_K$. Four combinations of $J$ and $K$ appear:

$$\begin{aligned}\Gamma_{\rm ent}^{00}=4mk\Bigg[&(T_{\upsilon0}^{\mu0}T_{\nu0}^{e0})^2+\frac{2h}{3}T_{\upsilon0}^{\mu0}T_{\nu0}^{e0}T_{\upsilon0}^{\mu1}T_{\nu0_-}^{e1}\\&+\frac{7}{15}(hT_{\upsilon0}^{\mu1}T_{\nu0_-}^{e1})^2\Bigg],\\\Gamma_{\rm ent}^{01}=4mk\Bigg[&3(T_{\upsilon0}^{\mu0}T_{\nu1}^{e0})^2-\frac{2h}{3}T_{\upsilon0}^{\mu0}T_{\nu1}^{e0}T_{\upsilon0}^{\mu1}T_{\nu1_-}^{e1}\\&+\frac{1}{3}(hT_{\upsilon0}^{\mu1}T_{\nu1_-}^{e1})^2-\frac{8h}{15}T_{\upsilon0}^{\mu0}T_{\nu1}^{e0}T_{\upsilon0}^{\mu1}T_{\nu1_+}^{e1}\\&+\frac{8h^2}{45}T_{\upsilon0}^{\mu1}T_{\nu1_-}^{e1}T_{\upsilon0}^{\mu1}T_{\nu1_+}^{e1}+\frac{556}{105}(hT_{\upsilon0}^{\mu1}T_{\nu1_+}^{e1})^2\Bigg],\\\Gamma_{\rm ent}^{10}=4mk\Bigg[&3(T_{\upsilon1}^{\mu0}T_{\nu0}^{e0})^2-\frac{2h}{3}T_{\upsilon1}^{\mu0}T_{\nu0}^{e0}T_{\upsilon1}^{\mu1}T_{\nu0_-}^{e1}\\&+\frac{1}{3}(hT_{\upsilon1}^{\mu1}T_{\nu0_-}^{e1})^2\Bigg],\\\Gamma_{\rm ent}^{11}=4mk\Bigg[&9(T_{\upsilon1}^{\mu0}T_{\nu1}^{e0})^2+\frac{2h}{3}T_{\upsilon1}^{\mu0}T_{\nu1}^{e0}T_{\upsilon1}^{\mu1}T_{\nu1_-}^{e1}\\&+\frac{1}{3}(hT_{\upsilon1}^{\mu1}T_{\nu1_-}^{e1})^2-\frac{4h}{3}T_{\upsilon0}^{\mu0}T_{\nu1_-}^{e0}T_{\upsilon1}^{\mu1}T_{\nu1_+}^{e1}\\&+\frac{2}{3}(hT_{\upsilon1}^{\mu1}T_{\nu1_+}^{e1})^2\Bigg].\end{aligned} \tag{20}$$

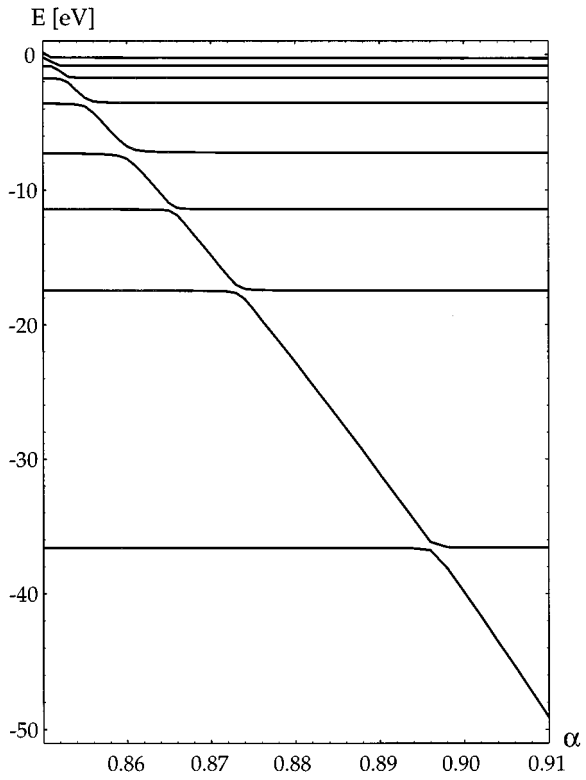


FIG. 3. Eigenvalues (eV) below the $t\mu(2s)$ threshold as a function of the scaling parameter $\alpha$. $N_{\text{bas}}=2700$, $J=0$.

Having five metastable states of each angular momentum $J$ situated within the Vesman formation region [12] we should investigate the magnitude of the matrix elements $T_{vJ}^{\mu L}$ and $T_{\nu K_{\pm}}^{eL}$ for each possible formation path. For this purpose, we need accurate energy levels and wave functions for the metastable $dt\mu^*$ molecule, as well as for the hybrid molecule $[(dt\mu^*)dee]_{\nu K}$.

### III. WAVE FUNCTIONS

The three-body wave functions $\Phi_{JM}(\boldsymbol{r},\boldsymbol{R})$ were obtained variationally by use of the coupled rearrangement channel method deviced by Kamimura [13]. $\Phi_{JM}$ is expanded in terms of Gaussian basis functions spanned over the three rearrangement channels shown in Fig. 2.

$$\Phi_{JM}=\sum_m c_m g_m$$

$$g_m=r^l R^L e^{-(r/r_i)^2} e^{-(R/R_I)^2}[Y_l(\hat{\boldsymbol{r}})\otimes Y_L(\hat{\boldsymbol{R}})]_{JM}. \quad (21)$$

The nonlinear variational parameters $r_i$ and $R_I$ are chosen as

$$r_i=r_1\left(\frac{r_n}{r_1}\right)^{(i-1)/(n-1)}, \quad R_I=R_1\left(\frac{R_N}{R_1}\right)^{(I-1)/(N-1)}. \quad (22)$$

The geometrical progression allows for an accurate description of both short- and long-range behavior.

Since the resonances sought for are embedded in the double scattering continuum of free $t\mu(1s)$ and $d\mu(1s)$ atoms, the Rayleigh-Ritz procedure will not yield absolute bounds of the resonance energies. Instead we apply the stabilization technique [7], where one introduces a real scaling parameter $\alpha$ through the transformations

$$r\rightarrow r\alpha, \quad T\rightarrow T/\alpha^2, \quad V\rightarrow V/\alpha, \quad (23)$$

where $T$ and $V$ are the kinetic and potential energy matrix elements, respectively. Varying $\alpha$ one obtains a stabilization graph as shown in Fig. 3.

Horizontal lines approximate the real part of resonance eigenvalues, while continuum eigenvalues will traverse $E$-space from above. Using up to 3000 basis functions we obtained stabilized eigenvalues for $J=0$ and $J=1$ as shown in Table I. Also given are the energies obtained with a direct inclusion of the first-order vacuum polarization potential [9].

The probability densities corresponding to pseudo wave functions $\chi_{vJ}(r_{dt})$ were obtained from $\Phi_{JM}$ by integrating over the muon coordinate in channel $c$;

$$|\chi_{vJ}(r_{dt})|^2=\int |\Phi_{JM}(\boldsymbol{r}_{dt},\boldsymbol{r}_{\mu})|^2 dr_{\mu} d\hat{\boldsymbol{r}}_{\mu} d\hat{\boldsymbol{r}}_{dt}. \quad (24)$$

Some examples are shown in Fig. 4. Note the irregular shape for binding energies less than 20 eV, arising from a strong mixing of the adiabatic $3\sigma$ and $4\sigma$ potentials. The Born-Oppenheimer classification used to enumerate the series of metastable states below the $n=2$ threshold in Refs. [4,5] as well as in Tables I and II thus will be adequate only for estimations of energy levels, not for wave-function-dependent properties such as lifetimes and transition matrix elements.

The matrix elements $T_{vJ}^{\mu L}$ were evaluated by approximating $\chi_{vJ}(r_{31})\simeq\chi_{vJ}(r_{dt})$, calculating the probability density in channel $c$ according to (24) and manually putting signs on consecutive lobes. Results in the limit $k\rightarrow 0$ are given in Table II.

TABLE I. Energies $E_b^{vJ}$ of $dt\mu^*$ resonances below the $t\mu(2s)$ threshold, given in eV. First column gives values obtained by assuming a pure Coulombic interaction $V_C$. The second is obtained when including the vacuum polarization potential $V_{\text{pol}}$ in the three-body Hamiltonian ($V_{\text{eff}}=V_C+V_{\text{pol}}$).

| $v$ | $E_b^{v0}(V_C)$ | $E_b^{v0}(V_{\text{eff}})$ | $E_b^{v1}(V_C)$ | $E_b^{v1}(V_{\text{eff}})$ |
|---|---|---|---|---|
| 0 | −217.889 | −217.829 | −212.543 | −212.480 |
| 1 | −139.728 | −139.642 | −135.362 | −135.271 |
| 2 | −79.119 | −79.013 | −75.673 | −75.565 |
| 3 | −36.619 | −36.501 | −34.237 | −34.117 |
| 4 | −17.463 | −17.341 | −16.336 | −16.213 |
| 5 | −7.251 | −7.138 | −6.482 | −6.360 |
| 6 | −3.578 | −3.458 | −3.187 | −3.068 |
| 7 | −1.732 | −1.614 | −1.514 | −1.397 |
| 8 | −0.832 | −0.718 | −0.713 | −0.601 |
| 9 | −0.396 | −0.288 | −0.324 | −0.219 |
| 10 | −0.181 | −0.087 | −0.146 | −0.060 |
| 11 | −0.070 | | −0.050 | |
| $4\sigma$ | −11.421 | −11.296 | −10.490 | −10.366 |
| $2\pi$ | | | −19.157 | −18.922 |

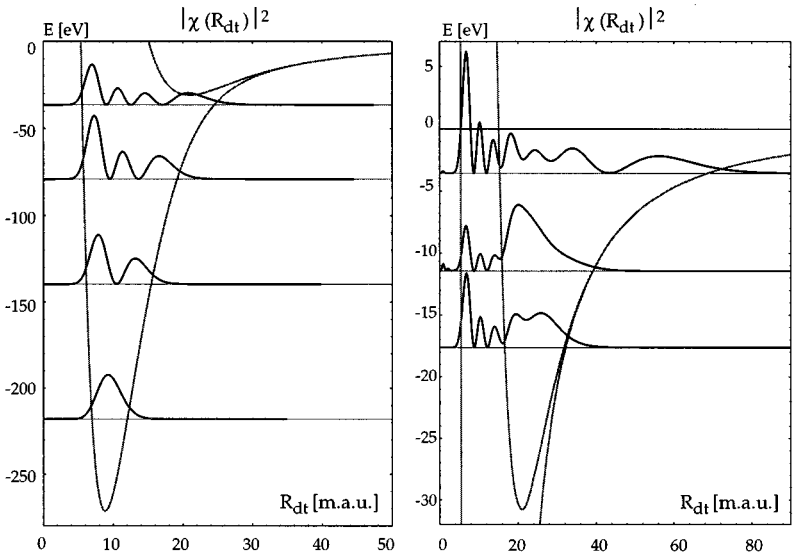


FIG. 4. $|\chi_{vJ}(r_{dt})|^2$ superimposed on the $3\sigma$ and $4\sigma$ potentials. $N_{\rm bas}=2700$, $J=0$.

Notice that even though the matrix element $\langle\chi_{vJ}(r_{31})|r_{31}\rangle$ grows with increasing $v$, the potential $V_{31}$ present in $T_{vJ}^{\mu L}$ introduces a ''cutoff'' that is manifested in the factor $E_b^{vJ}$ multiplying $\langle\chi_{vJ}(r_{31})|r_{31}\rangle$. Further, the inclusion of the vacuum polarization potential causes a shift in $E_b^{vJ}$, which suppresses the magnitude of $T_{vJ}^{\mu L}$ for high values of $v$. $\beta_{vJ}$ was estimated by observing that the shift $\Delta E$ obtained when evaluating the binding energies $E_b^{vJ}$ including the vacuum polarization potential, is related to the $2p$ orbital admixture in the $dt\mu^*$ wave function. We write $\beta^2\simeq 1-\Delta E/\Delta E_{2s}$, where $\Delta E_{2s}=0.236$ eV is the vacuum polarization shift of the free $t\mu(2s)$ atom and $\Delta E$ is derived from Table I. Comparing with the exact calculation of $\beta$ for $J=0$ made in [14], our estimation is in error by less than 2%.

The wave functions $\psi_{\nu K}$ were calculated in the Born-Oppenheimer approximation solving the one-dimensional Schrödinger equation for the nuclear motion

$$\left[\frac{d^2}{dR^2}-\frac{K(K+1)}{R^2}+2M[E_{\nu K}-V(R)]\right]u_{\nu K}(R)=0,$$

$$\psi_{\nu K}(R)=\frac{u_{\nu K}(R)}{R}, \tag{25}$$

using the nuclear potential calculated by Kolos and coworkers [15], the reduced mass $M$ being that of $D_2$ for the initial state, and that of $[(dt\mu)dee]$ for the final. The bound-state energies found agreed within 0.2 meV with values obtained by taking nonadiabatic effects into account [16]. Resulting $T_{\nu K}^{eL}$ in the limit $k\to 0$ are displayed in Table IV.

TABLE II. The matrix elements $T_{vJ}^{\mu L}$ for $dt\mu^*$ resonances associated with the first ten vibrational states of the adiabatic $3\sigma$ potential, calculated in the limit $k\to 0$. Also given are $T_{vJ}^{\mu J}$ for the single vibrational states associated with the $4\sigma$ and $2\pi$ potentials. Atomic units are assumed.

| $v$ | $\beta_{v0}$ | $T_{v0}^{\mu 0}$ | $\beta_{v1}$ | $T_{v1}^{\mu 1}$ |
|---|---|---|---|---|
| 0 | 0.864 | 0.0769 | 0.856 | 0.0042 |
| 1 | 0.797 | 0.0362 | 0.783 | 0.0032 |
| 2 | 0.742 | 0.0330 | 0.736 | 0.0030 |
| 3 | 0.707 | 0.0206 | 0.701 | 0.0027 |
| 4 | 0.695 | 0.0225 | 0.692 | 0.0033 |
| 5 | 0.722 | 0.0175 | 0.695 | 0.0054 |
| 6 | 0.701 | 0.0095 | 0.704 | 0.0050 |
| 7 | 0.707 | 0.0079 | 0.710 | 0.0044 |
| 8 | 0.719 | 0.0074 | 0.725 | 0.0053 |
| 9 | 0.736 | 0.0048 | 0.745 | 0.0046 |
| $4\sigma$ | 0.686 | 0.0176 | 0.689 | 0.0032 |
| $2\pi$ | | | 0.065 | 0.0001 |

## IV. THE REACTIVE WIDTH $\Gamma_r$

The first attempts to estimate Vesman formation rates for muonic molecules were not concerned with the nescessity of having a stabilizing process transferring the loosely bound state formed into a more tightly bound before the event of backdecay of the hybrid molecule [3]. Later it turned out that the reactive width $\Gamma_r$ appearing in the cross section (7) is essential for both qualitative and quantitative descriptions of the formation process.

In the present case, where a metastable state of $dt\mu$ is to be formed, $\Gamma_r$ has four components: the width $\Gamma_A$ for Auger transitions between metastable states, the fusion width $\Gamma_f$ for direct fusion of the particular state, $\Gamma_c$ representing the Coulombic lifetime of $dt\mu^*$, and $\Gamma_\gamma$ giving the rate of radiative decay.

A formalism for calculating $\Gamma_f$ for metastable states was developed in [7]. Preliminary extensions of those calculations indicate that $\Gamma_f$ for any of the states here concerned is less than $10^{10}$ s$^{-1}$.

The width for the radiative decay can be estimated by realizing that the muon of the $dt\mu^*$ molecule is strongly clustered on $t$, the deuteron only weakly interacting with the $t\mu$ atom. $\Gamma_\gamma$ is thus well approximated by the radiative decay rates of $t\mu(2s)$ and $t\mu(2p)$. For the $dt\mu^*$ states within the Vesman region, we have

$$\Gamma_\gamma=(1-\beta^2)\Gamma_\gamma^{2p\to 1s}(t\mu)\simeq 5\times 10^{10}\quad \mathrm{s}^{-1}. \tag{26}$$

The width for Coulombic decay was recently calculated by Kino and Kamimura to be $\simeq 10^{11}\ \mathrm{s}^{-1}$ [14], implying that the main contribution to the reactive width $\Gamma_r$ comes from the Auger transition

$$[(dt\mu^*)_{v_iJ_i}dee]\to[(dt\mu^*)_{v_fJ_f}de]^+ + e^-. \tag{27}$$

The width for (27) can be found from Fermi's golden rule,

$$\Gamma_A=2\pi\rho(E)\sum_f |\langle f|H_I|i\rangle|^2, \tag{28}$$

where $|f\rangle$ and $|i\rangle$ are final and initial states of the system and $\rho(E)$ is density of final states for a given energy. The interaction operator $H_I$ can be approximated by [17]

$$H_I=-\frac{\boldsymbol{r_e}\cdot\boldsymbol{d}}{r_e^3}, \tag{29}$$

where the dipole moment operator is

$$\boldsymbol{d}=\boldsymbol{r}_t+\boldsymbol{r}_d-\boldsymbol{r}_\mu \tag{30}$$

and $\boldsymbol{r}_e,\boldsymbol{r}_t,\boldsymbol{r}_d,\boldsymbol{r}_\mu$ are the particle coordinates with respect to the center of mass of $dt\mu^*$.

Writing the initial and final states as a product of the electronic and muonic wave functions and assuming that the density of final states is the same as for plane waves, $\rho(E)=2k/\pi$, (28) becomes

$$\Gamma_A=\frac{4k}{2J_i+1}\sum_M \left|\langle\Phi_f(\boldsymbol{r},\boldsymbol{R})|\boldsymbol{d}|\Phi_i(\boldsymbol{r},\boldsymbol{R})\rangle \times\left\langle \Psi_f(\boldsymbol{r_e})\left|\frac{\boldsymbol{r_e}}{r_e^3}\right|\Psi_i(\boldsymbol{r_e})\right\rangle\right|^2. \tag{31}$$

Here $\Phi(\boldsymbol{r},\boldsymbol{R})$ is the three-body wave function of $dt\mu^*$, in its initial and final state, and $\Psi(\boldsymbol{r}_e)$ is the wave function of the Auger electron being ejected from the hybrid molecule. The sum is to be taken over the magnetic quantum numbers $M_{J_i}$ and $M_{J_f}$.

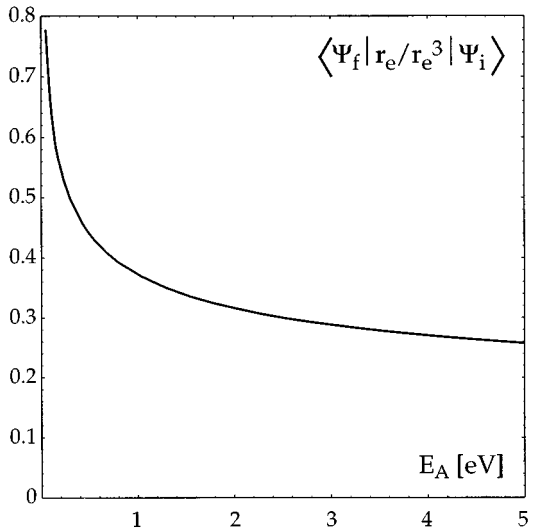


FIG. 5. The electronic matrix element $\langle\Psi_f|\mathbf{r}_e/\mathrm{r}_e^3|\Psi_i\rangle$ as function of the kinetic energy $E_A$ of the ejected Auger electron.

Rewriting the dipole operator as

$$\boldsymbol{d}=\boldsymbol{r}_{t\mu}+\frac{m_{t\mu}}{m_{t\mu}+m_d}\boldsymbol{r}_{31}, \tag{32}$$

we may use the fact that the muon of the $dt\mu^*$ molecule is strongly clustered on $t$ [14] to make the approximation $[r_{t\mu}<r_{dt}, a=m_{t\mu}/(m_{t\mu}+m_d), \beta^2\simeq 0.5$ for both initial and final states]

$$\langle\Phi_f(\boldsymbol{r},\boldsymbol{R})|\boldsymbol{d}|\Phi_i(\boldsymbol{r},\boldsymbol{R})\rangle \simeq\langle\chi_{v_fJ_f}(r_{dt})Y_{J_fM_{J_f}}(\hat{\boldsymbol{r}}_{dt})|a\boldsymbol{r}_{dt}|\chi_{v_iJ_i}(r_{dt})Y_{J_iM_{J_i}}(\hat{\boldsymbol{r}}_{dt})\rangle. \tag{33}$$

The electronic matrix element is calculated by taking the atomic wave functions

$$\Psi_i(\hat{\boldsymbol{r}}_e)=2e^{-r_e}Y_{00}(\hat{\boldsymbol{r}}_e)\Psi_f(\hat{\boldsymbol{r}}_e)=\frac{F_1(1/k;kr_e)}{kr_e}Y_{1M}(\hat{\boldsymbol{r}}_e) \tag{34}$$

as approximations for the actual two-center wave functions, $F_L$ being the regular Coulomb function. The wave number $k$ of the ejected electron is

$$k=\sqrt{2(\Delta E_b-E_I)}, \tag{35}$$

where $E_I=15.426$ eV is taken as the ionization threshold of $H_2$ [18] and $\Delta E_b=E_b^{vJ}-E_b^{v'J'}$.

The electronic matrix element as function of the kinetic energy $E_A=k^2/2$ of the Auger electron is displayed in Fig. 5. The radial part of the muonic matrix element for each transition of interest is given in Table III, with entries ordered with respect to increasing $E_A$. Note that the magnitude of the resulting width $\Gamma_A$ decreases as $E_A$ increases. It is found that the transition from the initial state $(v,J)=(8,0)$ has the largest width. This is partly due to the statistical factor $1/(2J_i+1)$, partly due to the spatial behavior of the wave functions $\chi_{vJ}$, featuring a pronounced $4\sigma$ component.

## V. EFFECTIVE FORMATION

Since the magnitude of cross section (7) is limited by the smallest of the widths $\Gamma_{\mathrm{ent}}$ and $\Gamma_r$, the effective formation rate can be quite different from $\Gamma_{\mathrm{ent}}$.

TABLE III. Radial muonic matrix elements $\langle\chi_f|ar_{dt}|\chi_i\rangle$ and widths $\Gamma_A$ for Auger transitions relevant to the $dt\mu^*$ formation process. Entries are ordered with respect to increasing $E_A$.

| $E_A$ (eV) | $v_i$ | $J_i$ | $v_f$ | $J_f$ | $\langle\chi_f\|ar_{dt}\|\chi_i\rangle$ | $\Gamma_A$ ($\mathrm{s}^{-1}$) |
|---|---|---|---|---|---|---|
| 0.069 | 8 | 0 | 4 | 1 | 0.024 | $7.6\times10^{13}$ |
| 0.518 | 7 | 1 | 4 | 0 | 0.031 | $4.2\times10^{13}$ |
| 0.549 | 9 | 0 | 4 | 1 | 0.010 | $4.2\times10^{13}$ |
| 1.314 | 8 | 1 | 4 | 0 | 0.020 | $1.8\times10^{13}$ |
| 1.518 | 9 | 1 | 4 | 0 | 0.021 | $2.0\times10^{13}$ |

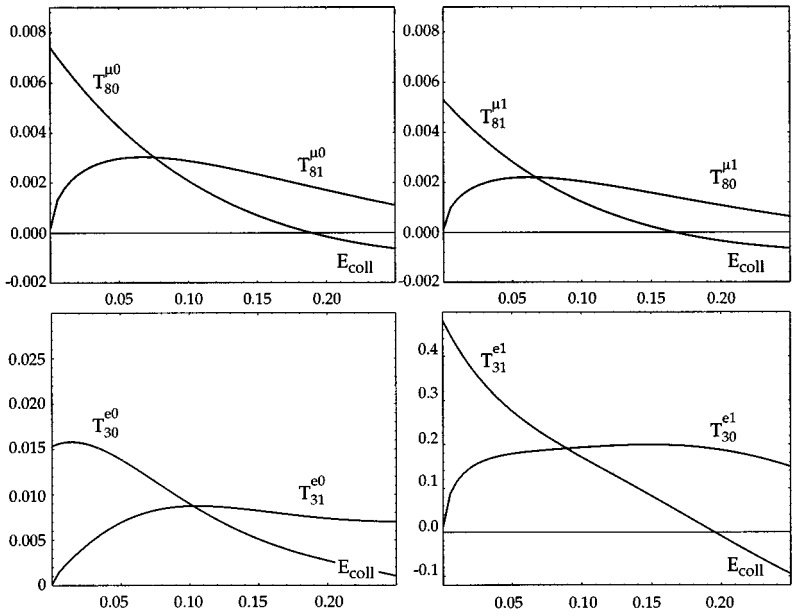


FIG. 6. The matrix elements $T_{8J}^{\mu L}$ and $T_{3K}^{eL}$ as a function of the center-of-mass collission energy $E_{\rm coll}$ (eV).

When comparing Tables I, II, IV, and III taking the energy conservation condition (8) into account, one finds that even though $\Gamma_{\rm ent}$ is largest for the formation configuration $v=9,\nu=1$ of angular momentum $J=1$ the most favorable configuration is for $v=8,\nu=3$ and $J=0$, with $E_b^{80}=0.718$ eV, which has the largest reactive width $\Gamma_r \simeq \Gamma_A$. Thus we evaluate the relevant matrix elements $T_{80}^{\mu L}$ and $T_{3K}^{eL}$ as function of the initial collision energy $E_{\rm coll}$, and display them in Fig. 6.

The concomitant entrance widths $\Gamma_{\rm ent}^{0K}$ are displayed in Fig. 7. We find that the entrance width is of the same order of magnitude as the width of the stabilizing Auger process.

We can now write the Breit-Wigner formula (7) for the cross section as

$$\sigma_{JK}(E_{\rm coll}) = \frac{\pi}{k^2} \frac{\Gamma_{\rm ent}^{JK}\Gamma_A}{(E_{\rm coll}-E_{\rm res}^{JK})^2 + \frac{1}{4}(\Gamma_{\rm ent}^{JK}+\Gamma_A)^2} \qquad (36)$$

where $E_{\rm res}^{JK}$ is the center-of-mass collision energy fulfilling the energy conservation condition for the particular formation path. Neglecting the difference of hyperfine levels at the $n=2$ level, we have $E_{\rm res}^{01}=0.159$ eV and $E_{\rm res}^{00}=0.154$ eV for the entrance widths given in Fig. 7. One must also consider the same resonances for $t\mu(2s)+DT$ collisions, where $\Gamma_{\rm ent}$ will be more or less identical, while $E_{\rm res}$ is shifted to $E_{\rm res}^{01}=0.079$ eV and $E_{\rm res}^{00}=0.074$ eV.

The cross sections for the four formation configurations thus appearing are displayed in Fig. 8. The collision energy dependence is quite different from what the Breit-Wigner formula usually provides, Fig. 8 not showing any sharp resonance peaks. This is beacause both $\Gamma_{\rm ent}$ and $\Gamma_A$ are of the same order of magnitude as $E_{\rm res}$, i.e., 0.1 eV. Thus the thermal distribution of $D_2$ energies that should be taken into account when transforming $\sigma^{0K}$ into the laboratory frame will not diminish the magnitude of the cross section as much as in the case of sharper peaks. It is important to realize that even though the cross sections have their maxima appearing at nonthermal energies, they will be accessible to $t\mu(2s)$ atoms with high kinetic energies. Measurements on the kinetic energy distribution of $p\pi$ atoms in excited states [19] have shown that a substantial fraction carried nonthermal energies, due to $n\rightarrow n'$ deexcitations in higher levels. It was

TABLE IV. Rovibrational energy levels $\overline{E_{\nu 1}}$ of the hybrid molecule $[(dt\mu)dee]$ assuming a pointlike $dt\mu$, which give transition energies $\Delta E_{\rm rovib}^{\nu 1}=\overline{E_{\nu 1}}-E_{00}$ with respect to the ground state of $D_2$, with $E_{00}=-4.556$ eV. The matrix elements $T_{\nu K}^{eL}$ are calculated in the limit $k\rightarrow 0$.

| $\nu$ | $\overline{E_{\nu 1}}$ | $\Delta E_{\rm rovib}^{\nu 1}$ | $T_{\nu 0}^{e0}$ | $T_{\nu 1}^{e1}$ |
|---|---|---|---|---|
| 0 | −4.5825 | −0.0265 | 0.998 | 0.041 |
| 1 | −4.2709 | 0.2851 | 0.023 | 3.501 |
| 2 | −3.9698 | 0.5862 | 0.059 | 0.527 |
| 3 | −3.6787 | 0.8773 | 0.015 | 0.472 |
| 4 | −3.3976 | 1.1584 | 0.009 | 0.227 |
| 5 | −3.1265 | 1.4295 | 0.005 | 0.157 |
| 6 | −2.8651 | 1.6909 | 0.003 | 0.079 |

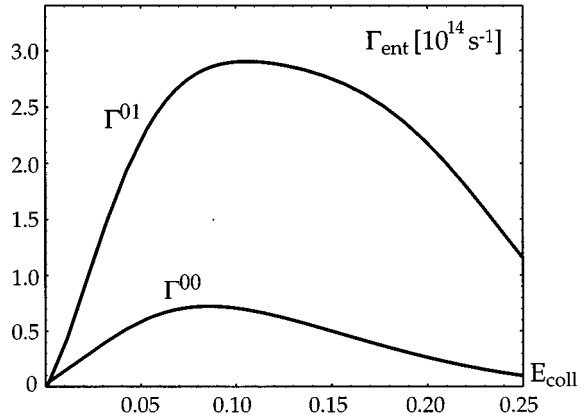


FIG. 7. $\Gamma_{\rm ent}^{0K}$ as a function of center-of-mass collision energy (eV), evaluated for $v=8,\nu=3$.

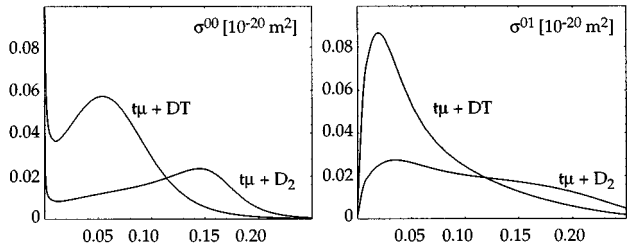


FIG. 8. The cross section $\sigma^{0K}(E_{\rm coll})$ for formation of $dt\mu^*$ in $t\mu(2s)+D_2$ and $t\mu(2s)+DT$ collisions, given as a function of center-of-mass collision energy (eV) and evaluated for $v=8,\nu=3,\Gamma_A=8\times10^{13}\ {\rm s}^{-1}$.

argued that as much as 50% of the exotic atoms would have kinetic energies above 1 eV when arriving to the ground state. This will most probably be the case also in the $\mu$CF cycle, meaning that the effective formation rate of $dt\mu^*$ will depend on the competition between thermalization and resonance formation. The effective formation rate $\lambda^{\rm eff}_{dt\mu^*}$ thus becomes time dependent:

$$\lambda^{JK}_{dt\mu^*}=\sum_X N_{DX}\rho v(E_{\rm coll})P(E_{\rm coll},t)\sigma^{JK}_{DX}(E_{\rm coll}), \quad (37)$$

where $N_{DX}$ is the fraction of $DX$ molecules, and $P(E,t)$ is the time-dependent distribution of collision energies. As $P(E,t)$ so far is not well known, apart from surely being different from the Maxwell distribution, we may not in the present paper give more than a rough estimation of $\lambda^{\rm eff}_{dt\mu^*}$ integrated over time. In order to find its order of magnitude we plot $\lambda^{JK}_{dt\mu^*}/P(E,t)$ In Fig. 9, which is seen to be approximately $0.5\times10^{11}\ {\rm s}^{-1}$ for $t\mu(2s)+DT$ collisions and slightly lower for $t\mu(2s)+D_2$ collisions. Keeping in mind that $\sigma^{JK}_{DX}$ is additive with respect to $J$ and $K$, and that there are a series of formation configurations that we have not treated explicitly, we estimate the resulting effective formation rate of $dt\mu^*$ to $\lambda^{\rm eff}_{dt\mu^*}\simeq10^{11}\ {\rm s}^{-1}$.

## VI. ENTRANCE WIDTHS FOR BOUND $dt\mu$

In order to assess the credibility of our results regarding $\Gamma_{\rm ent}$ we have used the present formalism to evaluate $\Gamma_{\rm ent}$ for the formation of the well-known bound states of $dd\mu$ and $dt\mu$.

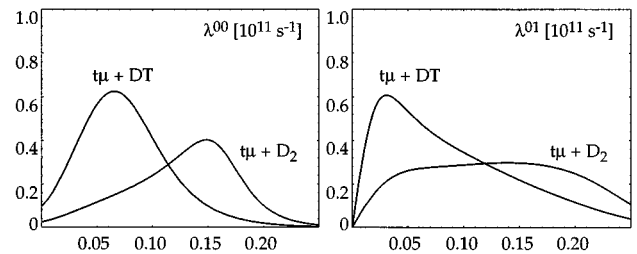


FIG. 9. The rate $\lambda^{JK}_{dt\mu^*}/P(E_c,t)$ for formation of $dt\mu^*$ in $t\mu(2s)+D_2$ and $t\mu(2s)+DT$ collisions, given as a function of center-of-mass collision energy (eV) and evaluated for $v=8,\nu=3$.

The loosely bound state of the $dd\mu$ molecule with $(v,J)=(1,1)$ has a binding energy of 1.966 eV, including relativistic corrections. It is formed in $d\mu(1s)-D_2$ collisions with the energy offset being absorbed by an excitation of the hybrid molecule $[(dd\mu)dee]_{\nu K}$ to its eight vibrational level $(\nu=7)$. As the vibrational wave function of the hybrid molecule has seven nodes, the overlap integral with the vibrational ground state of $D_2$ becomes small. One has

$$\langle\overline{\psi}_{7K_f}|\psi_{0K_i}(R)\rangle<0.01\left\langle\overline{\psi}_{7K_f}\left|\frac{d\psi_{0K_i}}{dR}\right.\right\rangle. \quad (38)$$

Thus the approximation

$$\nabla\Psi_{0K_i}(R)Y_{K_iM_{K_i}}(\hat{\boldsymbol{R}})\simeq\hat{\boldsymbol{R}}\frac{d\psi_{0K_i}}{dR}Y_{K_iM_{K_i}}(\hat{\boldsymbol{R}}) \quad (39)$$

becomes valid for all $K_i$. The matrix element $N(\boldsymbol{k})$ in Eq. (15) is now completely dominated by the second term.

Writing $\Gamma^{\mathcal{L}K_i\to JK_f}_{dd\mu}$ for the partial $\mathcal{L}$-wave contribution the following widths results for $i=0,1$ ($m$ being the reduced mass of $d\mu$ and $D_2$):

$$\Gamma^{10\to10}_{dd\mu}(k)=\frac{4mk}{3}(hT^{\mu1}_{11}T^{e1}_{70})^2,$$

$$\Gamma^{00\to11}_{dd\mu}(k)=\frac{4mk}{3}(hT^{\mu1}_{11}T^{e1}_{71})^2,$$

$$\Gamma^{01\to10}_{dd\mu}(k)=\frac{4mk}{3}\frac{1}{3}(hT^{\mu0}_{11}T^{eL}_{70})^2,$$

$$\Gamma^{11\to11}_{dd\mu}(k)=\frac{4mk}{3}\frac{6}{5}(hT^{\mu0}_{11}T^{eL}_{71})^2,$$

$$\Gamma^{01\to12}_{dd\mu}(k)=\frac{4mk}{3}\frac{2}{3}(hT^{\mu0}_{11}T^{eL}_{72})^2. \quad (40)$$

In the limit $k\to0$ transitions with $|K_i-K_f|\neq1$ are prohibited. The $K_i=0\to K_f=1$ transition is resonant at $E_{\rm res}=4.0$ meV [20] and is expected to dominate the primary formation of $dd\mu$ at low temperatures. In order to compare our $\Gamma^{00\to11}_{dd\mu}(k)$ with the results of Refs. [21,22] we plot the entity

$$\frac{\pi}{mk}\Gamma^{0i\to1f}_{dd\mu}\equiv|V_{if}|^2, \quad (41)$$

with $|V_{if}|^2$ defined by the equality. In Refs. [21–23] it was claimed that $V_{if}$, referred to as a ''transition matrix element,'' could be derived from perturbation theory. However, the resonance formation of a muonic molecule *leading to fusion* is a rearrangement process, for which pertubative treatments are not formally valid. The transition matrix element (1) for the full collision may indeed be rewritten in the ''post'' formulation as $T_{fi}=\langle\phi_f|V_f|\psi_i^{(-)}\rangle$, but then $V_f$ must be taken as the channel potential between the ejected Auger electron and the ionized complex, not as the interaction potential $\Delta V_{12}\equiv V_{12}(\boldsymbol{r}_{12})-V_{12}(\boldsymbol{R}_{31}-\boldsymbol{r}_2)$. As a matter of fact Lane has shown [11] that the channel potential $V_{31}$ by help of Green's theorem can be substituted by $\Delta V_{12}$, but then it is

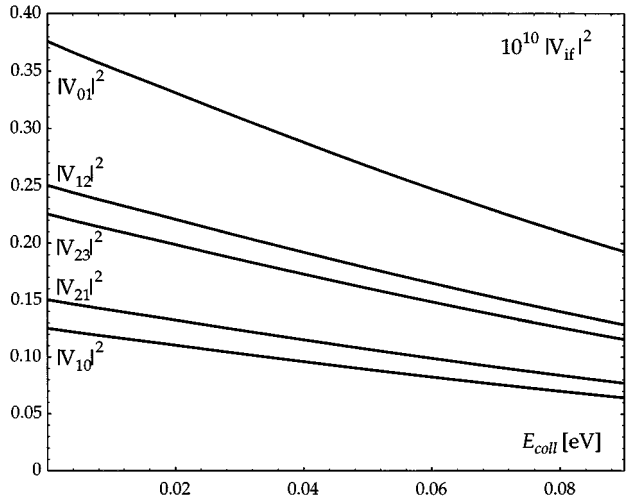


FIG. 10. The transition matrix element $|V_{if}|^2$ for formation of $dd\mu$ in $d\mu(1s)+D_2$ collisions. $|V_{if}|^2$ is given as function of the center-of-mass collision energy $E_{\rm coll}$ (eV) for $i=0,1,2$ and $|i-f|=1$.

still within the ''prior'' form of $T_{fi}$. This is also seen from the formal derivation of the Breit-Wigner formula (7) made by Armour [24].

Thus the formalism used by Faifman and Petrov is effectively equivalent to the one of Lane, although Faifman and Petrov start from an inconsistent scattering theoretic formulation. Actually, they use the alternative form $\Delta V_{12}$ of the channel potential $V_i=V_{31}$, which they incorrectly call the final interaction.

In conclusion, any difference in the resulting widths is due to different approximations of $\phi_i,\phi_r$ and the operator $V_i$. In the present paper, the Taylor expansion (13) of the initial wave function of the $D_2$ molecule is the major approximation, while the works of Faifman *et al.* [20,21] rely on a multipole expansion of the operator $\Delta_{12}$, using exact wave functions. As argued below, it turns out that the magnitude of the width is less sensitive to the quality of the $D_2$ wave function than to the interaction operator $\Delta V_{12}$.

To avoid the small incompatibility made by us in approximating $\chi(r_{dt})\simeq\chi(r_{31})$ when comparing to results of other authors, $T_{11}^{\mu 1}$ is evaluated by taking Menshikov's asymptotic formula [25] for the wave function $\chi_{11}$:

$$\chi_{11}=C\frac{1+\kappa r_{31}}{\sqrt{2\kappa r_{31}^2}}e^{-\kappa r_{31}} \tag{42}$$

with the constant $C=1.063$ calculated most recently in [26], and $\kappa=\sqrt{2mE_b}$. The integration in $T_{11}^{\mu 1}$ is made as suggested by Lane [11], with the part of the three-body integral that cannot be approximated by two-body functions ($r_{31}<0.05$) estimated to be 6% of the part where the asymptotic expression (42) is valid ($r_{31}>0.05$). The resulting energy dependence of $|V_{if}|^2$ for $i=0,1,2$ and $|K_i-K_f|=1$ is displayed in Fig. 10.

At $E_{\rm coll}=4$ meV we find $|V_{01}|^2=3.7\times10^{-11}$. Adjusting for the different values of $C$ used, $|V_{01}|^2$ given in [20,21] is larger by 58%. The discrepancy can be understood in the light of Ref. [22], where it was shown that the dipole approximation used in [20,21] overestimates $|V_{if}|^2$ by 55%.

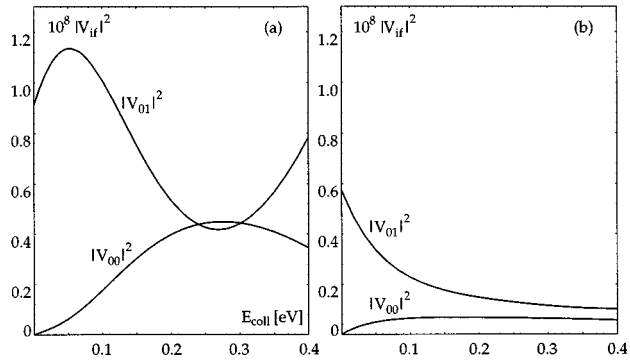


FIG. 11. The transition matrix element $|V_{0f}|^2$ for formation of $dt\mu$ in $t\mu(1s)+DH$ collisions (a) and $t\mu(1s)+D_2$ collisions (b). $|V_{0f}|^2$ is given as function of the center-of-mass collision energy $E_{\rm coll}$ (eV) for $f=0,1$.

Repeating the above evaluation for formation of $dt\mu$ molecules in $t\mu(1s)+D_2$ and $t\mu(1s)+DH$ collisions one finds that approximation (39) is *not* necessarily valid. The full expression (15) limited to $K_i=0$ must thus be used. If the spectator nucleus is a proton (DH), then the transitions $K_i=0$, $K_f=0,1$ have positive values of $E_{\rm res}$ for $\nu=2$. For $D_2$ the excitation of the hybrid molecule to $\nu=2$ can take place even for slightly negative values of $E_{\rm res}$, due to three-body collisions broadening a subthreshold resonance. This phenomenon is, however, beyond the scope of the present paper and we evaluate the entrance width relevant for positive resonances associated with excitation of the hybrid molecule to $\nu=3$. Using formulas (20) for the entrance width and the asymptotic formula (42) with $E_b=634.0$ meV (including relativistic corrections), and $C=0.874$ [26], for the $dt\mu$ wave function, the resulting matrix element $|V_{if}|^2$ is plotted in Fig. 11.

Comparing with the recent calculations [27], after adjusting for the different values of $C$ used, shows that the truncated Taylor expansion utilized by us gives decent results for formation configurations with $\nu=3$ $[t\mu(1s)+D_2]$. The discrepancy with Ref. [27] is 10% in this case, while for configurations with $\nu=2$ $[t\mu(1s)+DH]$ the terms left out by us yield an error of $\simeq 50\%$. Note that the matrix element $|V|^2$ given in [27] differs in definition from $|V_{if}|^2$ by a factor of 2.

We conclude that the Taylor expansion (14) has better convergence properties than the multipole expansion of [20,21], and can be used with some confidence for calculating formation rates of metastable $dt\mu^*$ accompanied by excitation of the hybrid molecule to $\nu=3$. We note that Menshikov's asymptotic formula is not well suited to approximate wave functions of $dt\mu^*$, making Petrov's method [22,27] difficult to apply to the present problem.

## VII. CONCLUSIONS

The cross section for the formation of $dt\mu^*$ resonances in $t\mu(2s)$-$D_2$ scattering was found to be limited by the rate of Auger deexcitations of the hybrid molecule $[(dt\mu^*)dee]$. The latter rate was found to be maximal for initial formation

of a state with angular momentum $J=0$ and a binding energy of 0.718 eV, having the value $\Gamma_A \simeq 8\times10^{13}\ \mathrm{s}^{-1}$. For this particular formation path, the cross section $\sigma^{JK}$ was in a wide range of collisions energies found to be approximately $0.02\times10^{-20}\ \mathrm{m}^2$ in $t\mu(2s)+D_2$ scattering and $0.05\times10^{-20}\ \mathrm{m}^2$ in $t\mu(2s)+DT$ scattering.

Among the approximations made, the Taylor expansion (14) of the initial $D_2$ wave function and the atomic wave functions taken for the ejected Auger electron are the most likely candidates to limit the accuracy of our results. Fortunately, the errors tend to cancel each other, as the former will yield slightly to large entrance widths, while the latter is expected to give too small rates for the Auger deexcitation. The series of formation configurations omitted by us will of course also contribute to the full cross section. In order to calculate the remaining terms one must take into account the correction to $dt\mu^*$ binding energies caused by interaction with the electrons of the hybrid molecule. Further, the effective formation rate will depend on the kinetic energy distribution of $t\mu(2s)$ atoms, which to large extent is unknown. Still we make the rough estimation that the effective formation rate of $dt\mu^*$ is of the order of $10^{11}\ \mathrm{s}^{-1}$.

## ACKNOWLEDGMENTS

J.W. would like to express his sincere gratitude to M. Kamimura for extending and explaining his method of calculating three-body wave functions during a stay at the Department of Physics of Kyushu University. In the same context, substantial financial support from the Japanese-German foundation in Berlin is acknowledged, as well as a generous allocation of CPU time at the supercomputing center of Kyushu University. P.F. is grateful for the continuous support from the Swedish Natural Research Council.

## APPENDIX A: DISCUSSION OF THE ENTRANCE WIDTH FORMULA

The entrance width can be obtained by considering the formation cross section expressed in terms of the transition amplitude. We start from the general expression

$$\Gamma=\hbar w \tag{A1}$$

connecting the entrance width with the transition rate $w$. The latter can be written as

$$w=J\sigma, \tag{A2}$$

where $\sigma$ is the (partial) cross section for the particular reaction, and $J$ is the flux of particles in the entrance channel, $J=(\hbar/m)\mathrm{Im}(\phi^*\nabla\phi)$. The latter is dependent on the normalization of the free waves describing the asymtotic motion of the reaction fragments. We set

$$\phi\equiv|\boldsymbol{k}\rangle=\frac{\exp(i\boldsymbol{k}\cdot\boldsymbol{r})}{(2\pi)^{3/2}}, \tag{A3}$$

which results in $J=[1/(2\pi)^3]v=\rho v$, with $v$ being the relative velocity of particles in the entrance channel, and $\rho$ their density.

The cross section for a given reaction, expressed in terms of the scattering amplitude, is [28]

$$\sigma_{ba}=\int d\Omega|f_{ba}|^2=\int d\Omega\,\frac{(2\pi)^4}{\hbar v_i}\,\frac{k_f m_f}{\hbar^2}|T_{ba}|^2, \tag{A4}$$

where $a,b$ denote the reaction channels, $m_i,k_i$, $m_f,k_f$ are the reduced masses and momenta of the relative motion in the initial and final states, respectively, and $T$ stands for the transition matrix element. The entrance width can now be obtained as

$$\begin{aligned}\Gamma_{ba}=\hbar\rho v_i\sigma_{ba}&=\hbar\rho\frac{\hbar k_i}{m_i}(2\pi)^4\frac{m_i m_f}{\hbar^4}\frac{k_f}{k_i}\int|T_{ba}|^2 d\Omega\\&=\rho(2\pi)^4\frac{m_f k_f}{\hbar^2}\int|\langle\psi_f^{(-)}|V_i|\boldsymbol{k}_i\rangle|^2 d\Omega\\&=\frac{4m_f k_f}{\hbar^2(4\pi)^2}\int|\langle\psi_f^{(-)}|V_i|e^{i\boldsymbol{k}_i\boldsymbol{r}}\rangle|^2 d\Omega,\end{aligned} \tag{A5}$$

which is the entrance width formula used in Sec. II.

## APPENDIX B: REDUCTION OF THE MATRIX ELEMENT INVOLVING $V_{13}$

We will now discuss the evaluation of the transition matrix elements involving the potential $V_{13}$. The integral to be calculated is in the $\boldsymbol{r}_{13}$ space and its calculation is facilitated by the following relations valid for the $d,t\mu$ subsystem:

$$H\Phi(\boldsymbol{r}_a,\boldsymbol{R}_a)=E\Phi(\boldsymbol{r}_a,\boldsymbol{R}_a), \tag{B1}$$

$$H'\,\eta e^{i\boldsymbol{k}\cdot\boldsymbol{R}_a}=E'\,\eta e^{i\boldsymbol{k}\cdot\boldsymbol{R}_a}, \tag{B2}$$

where $H$ is the complete Hamiltonian for $dt\mu$, $H'=H-V_{d\mu}-V_{dt}$ is the channel Hamiltonian defined by the interactions $V_{d\mu},V_{dt}$ between the deuteron and the $t\mu$ atom. $\Phi(\boldsymbol{r}_a,\boldsymbol{R}_a)$ is an eigenfunction to the total Hamiltonian $H$ expressed in the rearrangement channel $a$ of the Jacobi coordinates (see Fig. 2), whereas $\eta$ is an eigenfunction to the atomic Hamiltonian, satisfying $H_{t\mu}\eta=E^{t\mu}\eta$.

Noting that $H-H'=V_{d\mu}+V_{dt}=V_{13}$, and remembering that $\boldsymbol{R}_a\equiv\boldsymbol{r}_{13}$, $\boldsymbol{r}_a\equiv\boldsymbol{r}_{t\mu}$ one gets

$$\begin{aligned}\langle\Phi(\boldsymbol{r}_{13},\boldsymbol{r}_{t\mu})|V_{13}|\,\eta e^{i\boldsymbol{k}\cdot\boldsymbol{r}_{13}}\rangle&=\langle\Phi(\boldsymbol{r}_a,\boldsymbol{R}_a)|H-H'|\,\eta e^{i\boldsymbol{k}\cdot R_a}\rangle\\&=\langle\Phi(\boldsymbol{r}_a,\boldsymbol{R}_a)|E-E'|\,\eta e^{i\boldsymbol{k}\cdot R_a}\rangle\\&=(E-E')\langle\Phi(\boldsymbol{r}_{13},\boldsymbol{r}_{t\mu})|\,\eta e^{i\boldsymbol{k}\cdot\boldsymbol{r}_{13}}\rangle,\end{aligned} \tag{B3}$$

where $E-E'=E-E^{t\mu}-k^2/2\overline{m}$. For small collision energies, one has $E-E'\simeq E-E^{t\mu}\equiv E_b^{vJ}$. An approximation of the above matrix element, written in terms of the pseudo wave functions corresponding to $\Phi(\boldsymbol{r}_{13},\boldsymbol{r}_{t\mu})$ and $\eta e^{i\boldsymbol{k}\cdot\boldsymbol{r}_{31}}$ is given by

$$\begin{aligned}\langle\Phi(\boldsymbol{r}_{13},\boldsymbol{r}_{t\mu})|V_{13}|\,\eta e^{i\boldsymbol{k}\cdot\boldsymbol{r}_{13}}\rangle=E_b^{vJ}\langle\Phi(\boldsymbol{r}_{13},\boldsymbol{r}_{t\mu})|\,\eta\rangle_{r_{t\mu}}\langle\chi_v(r_{13})\\\times Y_{JM_J}(\hat{r}_{13})|e^{i\boldsymbol{k}\cdot\boldsymbol{r}_{13}}\rangle,\end{aligned} \tag{B4}$$

which is the relation (17) used in the main text.

We notice that the introduction of pseudo wave functions [for definition see Eq. (24)] leads to a significant simplification allowing practical evaluation of the transition matrix element defining the entrance width. It reduces the description of $D_2$ colliding with a composite particle $(t\mu)$ to one involving only the mass center of $t\mu$ implicitly interacting with the target via the correct potential $V_{31}=V_{dt}+V_{d\mu}$.

## APPENDIX C: THE TRANSITION MATRIX ELEMENT $N(k)$

In the present paper, the entrance width for formation of $dt\mu^*$ resonances at low temperatures is approximated by

$$\Gamma_{\rm ent}=\frac{4m_i k_i}{(4\pi)^2}\sum_M \int d\hat{\boldsymbol{k}}_i |N(\boldsymbol{k}_i)|^2, \tag{C1}$$

where $N(\boldsymbol{k}_i)$ is the matrix element

$$\begin{aligned} N(\boldsymbol{k}) \simeq & \langle \chi_v(r) Y_{JM_J}(\hat{\boldsymbol{r}}) | V_{31} | e^{if\boldsymbol{k}\cdot\boldsymbol{r}} \rangle \langle \overline{\psi_\nu}(R) Y_{KM_K}(\hat{\boldsymbol{R}}) | \psi_0(R) Y_{00}(\hat{\boldsymbol{R}}) e^{ig\boldsymbol{k}\cdot\boldsymbol{R}} \rangle \\ & - h \langle \chi_v(r) Y_{JM_J}(\hat{\boldsymbol{r}}) | V_{31} | \boldsymbol{r} e^{if\boldsymbol{k}\cdot\boldsymbol{r}} \rangle \cdot \left\langle \overline{\psi_\nu}(R) Y_{KM_K}(\hat{\boldsymbol{R}}) \middle| \hat{\boldsymbol{R}} \frac{\partial \psi_0}{\partial R} Y_{00}(\hat{\boldsymbol{R}}) e^{ig\boldsymbol{k}\cdot\boldsymbol{R}} \right\rangle . \end{aligned} \tag{C2}$$

The evaluation of (53) is simplified by use of the spherical vector components:

$$\hat{\boldsymbol{R}} = \sqrt{\frac{4\pi}{3}} [Y_{11}(\hat{\boldsymbol{R}}), Y_{10}(\hat{\boldsymbol{R}}), Y_{1-1}(\hat{\boldsymbol{R}})],$$

$$\hat{\boldsymbol{r}} = \sqrt{\frac{4\pi}{3}} [Y_{11}(\hat{\boldsymbol{r}}), Y_{10}(\hat{\boldsymbol{r}}), Y_{1-1}(\hat{\boldsymbol{r}})]. \tag{C3}$$

The plane-wave expansions

$$e^{if\boldsymbol{k}\cdot\boldsymbol{r}} = 4\pi \sum_L \sum_{M_L} i^L j_L(fkr) Y_{LM_L}(\hat{\boldsymbol{r}}) Y^*_{LM_L}(\hat{\boldsymbol{k}}), e^{ig\boldsymbol{k}\cdot\boldsymbol{R}} = 4\pi \sum_{\mathcal{L}} \sum_{M_{\mathcal{L}}} i^{\mathcal{L}} j_{\mathcal{L}}(gkR) Y_{\mathcal{L}M_{\mathcal{L}}}(\hat{\boldsymbol{R}}) Y^*_{\mathcal{L}M_{\mathcal{L}}}(\hat{\boldsymbol{k}}) \tag{C4}$$

then facilitate separation of radial and angular parts:

$$\begin{aligned} N(\boldsymbol{k}) = & (4\pi)^2 \left[ \sum_L \sum_{M_L} \langle \chi_v(r) | V_{31} | j_L(fkr) \rangle i^L Y^*_{LM_L}(\hat{\boldsymbol{k}}) \langle Y_{JM_J}(\hat{\boldsymbol{r}}) | Y_{LM_L}(\hat{\boldsymbol{r}}) \rangle \right] \\ & \times \left[ \sum_{\mathcal{L}} \sum_{M_{\mathcal{L}}} \langle \overline{\psi_\nu}(R) | \psi_0(R) j_{\mathcal{L}}(gkR) \rangle i^{\mathcal{L}} Y^*_{\mathcal{L}M_{\mathcal{L}}}(\hat{\boldsymbol{k}}) \langle Y_{KM_K}(\hat{\boldsymbol{R}}) | Y_{00}(\hat{\boldsymbol{R}}) Y_{\mathcal{L}M_{\mathcal{L}}}(\hat{\boldsymbol{R}}) \rangle \right] \\ & - \frac{(4\pi)^3}{3} h \left[ \sum_L \sum_{M_L} \langle \chi_v(r) | V_{31} | r j_L(fkr) \rangle i^L Y^*_{LM_L}(\hat{\boldsymbol{k}}) \langle Y_{JM_J}(\hat{\boldsymbol{r}}) | [Y_{11}(\hat{\boldsymbol{r}}), Y_{10}(\hat{\boldsymbol{r}}), Y_{1-1}(\hat{\boldsymbol{r}})] Y_{LM_L}(\hat{\boldsymbol{r}}) \rangle \right] \\ & \cdot \left[ \sum_{\mathcal{L}} \sum_{M_{\mathcal{L}}} \left\langle \overline{\psi_\nu}(R) \middle| j_{\mathcal{L}}(gkR) \frac{\partial \psi_0}{\partial R} \right\rangle i^{\mathcal{L}} Y^*_{\mathcal{L}M_{\mathcal{L}}}(\hat{\boldsymbol{k}}) \langle Y_{KM_K}(\hat{\boldsymbol{R}}) | [Y_{11}(\hat{\boldsymbol{R}}), Y_{10}(\hat{\boldsymbol{R}}), Y_{1-1}(\hat{\boldsymbol{R}})] Y_{00}(\hat{\boldsymbol{R}}) Y_{\mathcal{L}M_{\mathcal{L}}}(\hat{\boldsymbol{R}}) \rangle \right]. \end{aligned} \tag{C5}$$

Composition relations for the spherical harmonics yield the general formula

$$\begin{aligned} N(\boldsymbol{k}) = & (4\pi)^{3/2} [\langle \chi_v(r) | V_{31} | j_J(fkr) \rangle i^J Y^*_{JM_J}(\hat{\boldsymbol{k}}) \langle \overline{\psi_\nu}(R) | \psi_0(R) j_K(gkR) \rangle i^K Y^*_{KM_K}(\hat{\boldsymbol{k}})] \\ & - (4\pi)^{3/2} h \left( \sum_L \sum_{M_L} \langle \chi_v(r) | V_{31} | r j_L(fkr) \rangle i^L Y^*_{LM_L}(\hat{\boldsymbol{k}}) \left[ \begin{pmatrix} J & 1 & L \\ -M_J & -1 & M_L \end{pmatrix}, \begin{pmatrix} J & 1 & L \\ -M_J & 0 & M_L \end{pmatrix}, \begin{pmatrix} J & 1 & L \\ -M_J & 1 & M_L \end{pmatrix} \right] \right) \\ & \cdot \left( \sum_{\mathcal{L}} \sum_{M_{\mathcal{L}}} \left\langle \overline{\psi_\nu}(R) \middle| j_{\mathcal{L}}(gkR) \frac{\partial \psi_0}{\partial R} \right\rangle i^{\mathcal{L}} Y^*_{\mathcal{L}M_{\mathcal{L}}}(\hat{\boldsymbol{k}}) \left[ \begin{pmatrix} J & 1 & \mathcal{L} \\ -M_K & -1 & M_{\mathcal{L}} \end{pmatrix}, \begin{pmatrix} K & 1 & \mathcal{L} \\ -M_K & 0 & M_{\mathcal{L}} \end{pmatrix}, \begin{pmatrix} K & 1 & \mathcal{L} \\ -M_K & 1 & M_{\mathcal{L}} \end{pmatrix} \right] \right). \end{aligned} \tag{C6}$$

[1] P. Froelich, Adv. Physics **41**, 405 (1992).
[2] G. Fesenko and G. Korenman, Muon Catalyzed Fusion **6**, 495 (1990).
[3] E. Vesman, Pis'ma Zh. Eksp. Teor. Fiz. **5**, 113 (1967) [JETP Lett. **5**, 91, (1967)].
[4] S. Hara and T. Ishihara, Phys. Rev. A **40**, 4232 (1989).
[5] I. Shimamura, Phys. Rev. A **40**, 4863 (1989).
[6] P. Froelich, A. Flores, and S. Alexander, Phys. Rev. A **40**, 2330 (1992).
[7] P. Froelich and A. Flores, Phys. Rev. Lett. **70**, 1595 (1993).
[8] P. Froelich and J. Wallenius, Phys. Rev. Lett. **75**, 2108 (1995).
[9] J. Wallenius and P. Froelich, Phys. Lett. A **206**, 73 (1995).
[10] J. Taylor, *Scattering Theory* (Wiley, New York, 1972).
[11] A. Lane, J. Phys. B **21**, 2159 (1988).
[12] J. Wallenius and M. Kamimura, in Proceedings of the International Workshop on Muon Catalyzed Fusion in Dubna, 1995, edited by L. Ponomarev [HyperFine Interact. (to be published)].
[13] M. Kamimura, Phys. Rev. A **38**, 621 (1988).
[14] Y. Kino and M. Kamimura, in Proceedings of the International Workshop on Muon Catalyzed Fusion in Dubna, 1995, edited by L. Ponomarev [HyperFine Interact. (to be published)].
[15] W. Kolos, K. Szalewicz, and H. Monkhorst, J. Chem. Physics **84**, 3276 (1986).
[16] A. Scrinzi, K. Szalewicz, and H. Monkhorst, Phys. Rev. A **37**, 2270 (1988).
[17] A. Scrinzi and K. Szalewicz, Phys. Rev. A **39**, 2855 (1989).
[18] G. Herzberg, Phys. Rev. Lett. **23**, 1081 (1969).
[19] E. Aschenauer *et al.*, Phys. Rev. A **51**, 1965 (1995).
[20] A. Scrinzi *et al.*, Phys. Rev. A **47**, 4691 (1993).
[21] M. Faifman, L. Menshikov, and T. Strizh, Muon Catalyzed Fusion **4**, 1 (1989).
[22] Y. Petrov and V. Petrov, Zh. Eksp. Teor. Fiz. **100**, 56 (1991) [Sov. Phys. JETP **73**, 29 (1991)].
[23] L. Menshikov and M. Faifman, Yad. Fiz. **43**, 650 (1986) [Sov. J. Nucl. Phys. **43**, 414 (1986)].
[24] E. Armour, J. Phys. B **27**, L763 (1994).
[25] L. Menshikov, Yad. Fiz. **42**, 1184 (1985) [Sov. J. Nucl. Phys. **42**, 750 (1985)].
[26] Y. Kino *et al.*, Phys. Rev. A **52**, 870 (1995).
[27] Y. Petrov, V. Petrov, and H. Schmidt, Phys. Lett. B **331**, 266 (1994).
[28] C. Joachin, *Collision Theory* (Springer, Berlin, 1975).